J. Fluid Mech. (2015), *vol.* 765, *pp.* 150–166.
doi:10.1017/jfm.2014.728

Linear stability analysis of a premixed flame with transverse shear

Xiaoyi Lu[1,†] **and Carlos Pantano**[1]

[1]Department of Mechanical Science and Engineering, University of Illinois at Urbana-Champaign, Urbana, IL 61801, USA

(Received 4 September 2014; revised 5 December 2014; accepted 12 December 2014; first published online 19 January 2015)

One-dimensional planar premixed flames propagating in a uniform flow are susceptible to hydrodynamic instabilities known (generically) as Darrieus–Landau instabilities. Here, we extend that hydrodynamic linear stability analysis to include a lateral shear. This generalization is a situation of interest for laminar and turbulent flames when they travel into a region of shear (such as a jet or shear layer). It is shown that the problem can be formulated and solved analytically and a dispersion relation can be determined. The solution depends on a shear parameter in addition to the wavenumber, thermal expansion ratio, and Markstein lengths. The study of the dispersion relation shows that perturbations have two types of behaviour as wavenumber increases. First, for small shear, we recover the Darrieus–Landau results except for a region at small wavenumbers, large wavelengths, that is stable. Initially, increasing shear has a stabilizing effect. But, for sufficiently high shear, the flame becomes unstable again and its most unstable wavelength can be much smaller than the Markstein length of the zero-shear flame. Finally, the stabilizing effect of low shear can make flames with negative Markstein numbers stable within a band of wavenumbers.

Key words: flames, instability, reacting flows

1. Introduction

Premixed flames are unstable to perturbations owing to gas expansion effects in what is called the Darrieus–Landau or hydrodynamic instability (DL) (Darrieus 1938; Landau 1945). There have been numerous analytical, numerical and experimental studies of premixed flames. The basic configuration corresponds to a nominally planar flame propagating against a mixture of reactants (or stabilized by an opposing flow matching the flame speed). Apart from the DL instability, flames can be unstable owing to thermo-diffusive effects (different diffusivity of heat and mass) (Sivashinsky 1976; Clavin & Williams 1982; Matalon & Matkowsky 1982; Pelcé & Clavin 1982), flow interaction (Buckmaster 1977; Matalon 1983; Searby & Clavin 1986), and heat loss to walls and gravity (Joulin & Sivashinsky 1994). The most amplified wavenumber depends, among other things, on the stabilizing role of curvature and strain (through diffusion) that can be parameterized in linear stability analysis by one or two length scales called the Markstein lengths (Markstein 1964; Clavin & Williams 1982; Clavin & Graña-Otero 2011), that are of the order of the preheat-zone

† Email address for correspondence: xlu19@illinois.edu

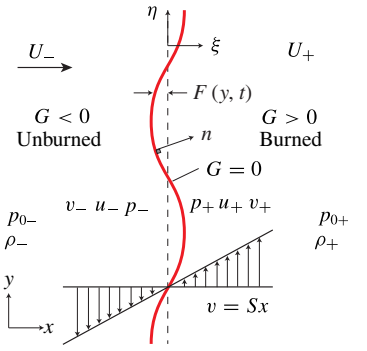

FIGURE 1. (Colour online) Sketch of flame configuration.

flame thickness. Furthermore, after the linear phase of instability one encounters a nonlinear phase where the amplitude of the flame stabilizes (Sivashinsky 1977, 1990; Creta & Matalon 2011*a*). Further reviews on laminar and turbulent premixed flames can be found in Sivashinsky (1983), Matalon (2007), Driscoll (2008) and Lipatnikov & Chomiak (2010).

Analytical studies can start with the so-called hydrodynamic limit where the stability properties of the flame can be explained quite accurately by ignoring the internal structure of the flame and considering it as an infinitesimally thin jump in density from the high value upstream of the flame to the low value downstream of the flame front. This works well for Lewis numbers close to unity, where the Lewis number is defined as the ratio of the thermal to the mass diffusivity of the species. The effect of non-uniformities in the incoming flow has been considered in numerous studies, e.g. Clavin & Williams (1982), Ashurst & Sivashinsky (1991), Berestycki & Sivashinsky (1991), Brailovsky & Sivashinsky (1993, 1995), Aldredge (1996), Kagan, Sivashinsky & Makhviladze (1998), Kortsarts *et al.* (1998), Audoly, Berestycki & Pomeau (2000), Kagan & Sivashinsky (2000). These studies considered essentially the effects induced by changes in the streamwise (flame normal) aligned velocity (some in the small perturbation limit, others nonlinearly). Here, we consider a new case where the flame tangential velocity is not uniform. This can occur when a flame propagates into a region of free shear flow. The purpose of this communication is the analytical description of the simplest situation: near unity Lewis numbers; no other flow but that induced by shear; and completely linear behaviour (early time). With sufficient extensions, this configuration may be useful in understanding more complex problems in turbulent premixed flames. Recent direct numerical simulations (DNS) by Hawkes *et al.* (2012), where a set of twin premixed flames propagate into a region of turbulence created by planar shear layers, are an example of such a flow.

2. Flame model and mathematical formulation

The hydrodynamic linear stability analysis assumes that a planar flame propagates at a constant speed in the direction normal to itself, which is counterbalanced by an opposite flow of premixed reactants. The problem configuration is illustrated in figure 1. This generalization has the feature that there is a transverse pressure gradient orthogonal to the density gradient and it has a background of constant (initial) vorticity. The flame is considered as an infinitesimally thin sheet where fast reaction occurs. Effects of buoyancy are neglected. Given these assumptions, the

only influence of combustion in this problem is thermal expansion of the flow and the consequential discontinuities of thermal properties. As is well known, thermal expansion deflects the downstream streamlines from the parallel upstream streamlines incoming towards the flame. The downstream streamlines are also parallel far from the flame. The present configuration is a generalization of the classical Darrieus–Landau problem. The present extension incorporates a transverse shear flow parallel to the flame plane which can be described analytically by $v = Sx$, where S is a constant. This flow is still divergence free. The flame front is described by the implicit relation $G = x - F(y, t) = 0$ and the flame normal and local flame velocity in the case of small perturbation are given by

$$\boldsymbol{n} = \frac{\boldsymbol{\nabla} G}{|\boldsymbol{\nabla} G|} = \frac{1}{|\boldsymbol{\nabla} G|}\left(1, -\frac{\partial F}{\partial y}\right), \quad s_f = \frac{1}{|\boldsymbol{\nabla} G|}\frac{\partial F}{\partial t}, \tag{2.1a,b}$$

where $\boldsymbol{n}$ is the flame normal pointing towards the burned gases and s_f denotes the flame surface velocity. The flame front separates the neighbourhood of the flame into unburned (left) and burned (right) regions. Fluid properties of interest, including flow velocity u and v, pressure p, and density ρ, are denoted with subscripts $(\cdot)_-$ and $(\cdot)_+$ in unburned and burned gas regions, respectively. The thermal expansion ratio r is defined as the ratio of burned gas density to unburned gas density, and it is therefore less than unity. The local flame speed, s_L, is assumed given by

$$s_L = s_L^o\left(1 - \mathscr{L}\boldsymbol{\kappa} + \mathscr{L}_s \boldsymbol{n}\cdot\boldsymbol{\nabla}\boldsymbol{u}\cdot\boldsymbol{n}\right), \tag{2.2}$$

where s_L^o denotes the burning velocity of the laminar planar flame, κ denotes the curvature of the flame front, and $\mathscr{L}$ and $\mathscr{L}_s$ denote the Markstein lengths due to curvature and strain, respectively, see Clavin & Graña-Otero (2011). The Markstein lengths have a characteristic magnitude of the order of the laminar flame thickness.

In order to reduce the problem to its simplest form, quantities are non-dimensionalized using the laminar planar flame thickness l_F and burning velocity s_L^o, giving the following non-dimensional quantities:

$$\left.\begin{aligned} u^* &= \frac{u}{s_L^o}, \quad v^* = \frac{v}{s_L^o}, \quad p^* = \frac{p}{\rho_u s_L^{o2}}, \quad \rho^* = \frac{\rho}{\rho_u}, \quad \mathscr{M} = \frac{\mathscr{L}}{l_F}, \\ x^* &= \frac{x}{l_F}, \quad y^* = \frac{y}{l_F}, \quad t^* = \frac{t}{l_F/s_L^o}, \quad S^* = \frac{S l_F}{s_L^o}, \quad \mathscr{M}_s = \frac{\mathscr{L}_s}{l_F}. \end{aligned}\right\} \tag{2.3}$$

To simplify further the notation, we will drop the '*' superscript since it will not induce any confusion later. The results will depend on the Markstein numbers $\mathscr{M}$ and $\mathscr{M}_s$. Under this normalization, the flow velocity ahead of the flame is $U_- = 1$ and the density is $\rho_- = 1$, while behind the flame we have U_+ (to be determined below from the jump conditions) and $\rho_+ = r$.

The flow is governed by Euler's equations (in this inviscid approximation) at both sides of the flame sheet, such that

$$\frac{\partial u}{\partial x} + \frac{\partial v}{\partial y} = 0, \tag{2.4}$$

$$\frac{\partial u}{\partial t} + u\frac{\partial u}{\partial x} + v\frac{\partial u}{\partial y} = -\frac{1}{\rho}\frac{\partial p}{\partial x}, \tag{2.5}$$

$$\frac{\partial v}{\partial t} + u\frac{\partial v}{\partial x} + v\frac{\partial v}{\partial y} = -\frac{1}{\rho}\frac{\partial p}{\partial y}. \tag{2.6}$$

The pressure and velocity at either side of the flame are related by the corresponding jump conditions (Williams 1985), which are derived from conservation of mass and momentum across the flame, giving

$$(r-1)\frac{\partial F}{\partial t} = r\left(u_+ - \frac{\partial F}{\partial y}v_+\right) - \left(u_- - \frac{\partial F}{\partial y}v_-\right), \tag{2.7}$$

$$(ru_+ - u_-)\frac{\partial F}{\partial t} = ru_+\left(u_+ - \frac{\partial F}{\partial y}v_+\right) - u_-\left(u_- - \frac{\partial F}{\partial y}v_-\right) + p_+ - p_-, \tag{2.8}$$

$$(rv_+ - v_-)\frac{\partial F}{\partial t} = rv_+\left(u_+ - \frac{\partial F}{\partial y}v_+\right) - v_-\left(u_- - \frac{\partial F}{\partial y}v_-\right) - \frac{\partial F}{\partial y}(p_+ - p_-). \tag{2.9}$$

The main difference with classical Darrieus–Landau analysis is the presence of v terms which cannot be neglected from the outset. Using (2.7) for the flat flame reference conditions we obtain $U_+ = 1/r$. Then, one can obtain from the momentum conservation equations that $p_\pm = -Sy + p_{0\pm}$. Note that it is not known *a priori* that the shear at both sides of the flame, $S_\pm$, is the same, but one can verify that the jump conditions are solvable only if $S_- = S_+ = S$. The quantitative relation between constants of integration p_- and p_+ remains unknown. Given the equalities above, pressure terms can be used to substitute horizontal velocity terms into the jump conditions, (2.8), providing

$$\frac{1}{r} - 1 + p_{0+} - p_{0-} = 0. \tag{2.10}$$

If one sets the additive constant $p_{0-} = 0$, then p_{0+} is equal to $(r-1)/r$.

3. Perturbation analysis

Following the notation in Peters (2010) for the classical DL analysis, we introduce a perturbative expansion on a small parameter ϵ denoting the amplitude of a deformation in the original flat flame surface. The fields are now written as

$$u_- = 1 + \epsilon\hat{u}_- + O(\epsilon^2), \quad u_+ = \frac{1}{r} + \epsilon\hat{u}_+ + O(\epsilon^2), \tag{3.1a,b}$$

$$v_- = Sx + \epsilon\hat{v}_- + O(\epsilon^2), \quad v_+ = Sx + \epsilon\hat{v}_+ + O(\epsilon^2), \tag{3.2a,b}$$

$$p_- = -Sy + \epsilon\hat{p}_- + O(\epsilon^2), \quad p_+ = 1 - \frac{1}{r} - Sy + \epsilon\hat{p}_+ + O(\epsilon^2). \tag{3.3a,b}$$

Furthermore, we introduce a coordinate transformation to simplify the analysis, given by $x = \xi + F(\eta, \tau)$, $y = \eta$, and $t = \tau$. In this frame of reference, the flame surface $G = 0$ corresponds to $\xi = 0$. Finally, we write $F = \epsilon f + O(\epsilon^2)$ and take f to be a quantity of order one. Introducing these expansions in (2.4)–(2.6) results to first order in

$$\frac{\partial\hat{u}}{\partial\xi} + \frac{\partial\hat{v}}{\partial\eta} = 0, \tag{3.4}$$

$$\frac{\partial\hat{u}}{\partial\tau} + \frac{1}{r}\frac{\partial\hat{u}}{\partial\xi} + S\xi\frac{\partial\hat{u}}{\partial\eta} + \frac{1}{r}\frac{\partial\hat{p}}{\partial\xi} = 0, \tag{3.5}$$

$$\frac{\partial}{\partial\tau}\left(Sf+\hat{v}\right)+\frac{1}{r}\frac{\partial\hat{v}}{\partial\xi}+S\hat{u}+S\xi\frac{\partial\hat{v}}{\partial\eta}+\frac{1}{r}\frac{\partial\hat{p}}{\partial\eta}=0, \tag{3.6}$$

where $\hat{u}(\xi,\,\eta,\,r,\,\tau)$, $\hat{v}(\xi,\,\eta,\,r,\,\tau)$ and $\hat{p}(\xi,\,\eta,\,r,\,\tau)$ can be used to represent both solutions to the left and right of $\xi=0$: $\hat{u}_-=\hat{u}(\xi,\,\eta,\,1,\,\tau)$ for $\xi<0$ and $\hat{u}_+=\hat{u}(\xi,\,\eta,\,r,\,\tau)$ for $\xi>0$; and similarly for the other fields. Introducing the perturbation expansion in the jump conditions, one gets to first order (after evaluating the jump condition at $\xi=0$)

$$(r-1)\frac{\partial f}{\partial\tau}=r\hat{u}_+-\hat{u}_-, \tag{3.7}$$

$$0=2(\hat{u}_+-\hat{u}_-)+\hat{p}_+-\hat{p}_-, \tag{3.8}$$

$$0=\hat{v}_+-\hat{v}_--\left(1-\frac{1}{r}\right)\frac{\partial f}{\partial\eta}. \tag{3.9}$$

Note that most terms in the tangential velocity jump equation due to the presence of shear can be ignored because they are of higher order, just as happens in the premixed flame without shear (Matalon & Matkowsky 1982; Pelcé & Clavin 1982).

These equations are coupled with the kinematic equation of the flame surface, which requires

$$s_f=\boldsymbol{v}\cdot\boldsymbol{n}-s_L. \tag{3.10}$$

This condition is imposed using a level set equation, given by

$$\frac{\partial G}{\partial t}+\boldsymbol{v}\cdot\nabla G=s_L|\nabla G|, \tag{3.11}$$

where the flame velocity s_L incorporates the effects of curvature and strain, according to

$$s_L=1-\mathscr{M}\boldsymbol{\kappa}+\mathscr{M}_s\boldsymbol{n}\cdot\nabla u\cdot\boldsymbol{n}, \tag{3.12}$$

where $\boldsymbol{\kappa}$ denotes the curvature of the flame, $\boldsymbol{\kappa}=-\nabla\cdot\boldsymbol{n}$. With all these elements, we obtain

$$\frac{\partial G}{\partial t}+u\frac{\partial G}{\partial x}+v\frac{\partial G}{\partial y}=(1-\mathscr{M}\boldsymbol{\kappa}+\mathscr{M}_s\boldsymbol{n}\cdot\nabla u\cdot\boldsymbol{n})\sqrt{\left(\frac{\partial G}{\partial x}\right)^2+\left(\frac{\partial G}{\partial y}\right)^2}. \tag{3.13}$$

Introducing the perturbation expansion, we obtain to first order in ϵ, the following boundary condition:

$$\hat{u}_-|_{\xi=0}=\frac{\partial f}{\partial\tau}-\mathscr{M}\frac{\partial^2 f}{\partial\eta^2}+\mathscr{M}_s\left(\left.\frac{\partial\hat{u}_-}{\partial\xi}\right|_{\xi=0}-S\frac{\partial f}{\partial\eta}\right). \tag{3.14}$$

4. Solution and dispersion relation

We now seek a general solution of the above equations and boundary condition of the form

$$\psi=\tilde{\psi}(\xi)\exp(\sigma\tau-\mathrm{i}k\eta), \tag{4.1}$$

where ψ denotes any of the unburned or burned side fields ($\hat{u}_\pm$, $\hat{v}_\pm$, $\hat{p}_\pm$) and

$$f=\tilde{f}\exp(\sigma\tau-\mathrm{i}k\eta). \tag{4.2}$$

The parameter σ is termed here the amplification factor and k denotes the wavenumber of the perturbation. The system of seven linear differential equations is closed for

$\tilde{u}_\pm$, $\tilde{v}_\pm$, $\tilde{p}_\pm$ and $\tilde{f}$, giving

$$\frac{\mathrm{d}\tilde{u}}{\mathrm{d}\xi} - \mathrm{i}k\tilde{v} = 0, \tag{4.3}$$

$$(\sigma - \mathrm{i}kS\xi)\tilde{u} + \frac{1}{r}\frac{\mathrm{d}\tilde{u}}{\mathrm{d}\xi} + \frac{1}{r}\frac{\mathrm{d}\tilde{p}}{\mathrm{d}\xi} = 0, \tag{4.4}$$

$$S\sigma\tilde{f} + \tilde{u}S + (\sigma - \mathrm{i}kS\xi)\tilde{v} + \frac{1}{r}\frac{\mathrm{d}\tilde{v}}{\mathrm{d}\xi} - \mathrm{i}k\frac{1}{r}\tilde{p} = 0, \tag{4.5}$$

with the boundary condition

$$\tilde{u}_-|_{\xi=0} - \mathscr{M}_s\frac{\partial\hat{u}_-}{\partial\xi}\bigg|_{\xi=0} = (\sigma + \mathscr{M}k^2 + \mathrm{i}k\mathscr{M}_sS)\tilde{f}. \tag{4.6}$$

The general solution of $\tilde{u}(\xi, r)$ can be obtained from this closed system of differential equations by eliminating $\tilde{v}$ (using (4.3)) and $\tilde{p}$ (using (4.5)) and has the general form

$$\tilde{u}(\xi, r) = c_1\mathrm{e}^{-k\xi} + c_2\mathrm{e}^{k\xi} + c_3\left\{\mathrm{e}^{-k\xi}\mathrm{erfi}[g_-(\xi)] - \mathrm{e}^{k\xi+2\mathrm{i}(\sigma/S)}\mathrm{erfi}[g_+(\xi)]\right\}, \tag{4.7}$$

where

$$g_\pm(\xi) = (1+\mathrm{i})\,\frac{k(\xi rS \pm \mathrm{i}) + \mathrm{i}r\sigma}{2\sqrt{krS}}, \tag{4.8}$$

and $\mathrm{erfi}(z) = -\mathrm{i}\,\mathrm{erf}(\mathrm{i}z)$ denotes the imaginary error function (an entire function). Note that r is retained as an independent parameter in the function $\tilde{u}$ in order to represent both solutions $\tilde{u}_-$ (when setting $r = 1$) and $\tilde{u}_+$. The constants $c_{1\pm}$, $c_{2\pm}$ and $c_{3\pm}$ at both sides of the flame must be determined by requiring that perturbations vanish as $|\xi| \to \infty$. From the properties of $\mathrm{erfi}(z)$ for large z, we have

$$\mathrm{erfi}(z) \sim \mathrm{i}\,\mathrm{sgn}(\mathrm{Re}(z)) + \frac{\mathrm{e}^{z^2}}{\sqrt{\pi}z} \quad \text{for } z \to \infty. \tag{4.9}$$

This implies that $c_{1-} = c_{3-} = 0$ and $c_{2+} = \mathrm{i}\mathrm{e}^{2\mathrm{i}\sigma/S}c_{3+}$. The complete solution is cumbersome to write but it can be evaluated at $\xi = 0$ easily and combined with (3.7)–(3.9) to form a linear system of equations for the free parameters c_{2-}, c_{1+} and c_{3+}. In order for this system to have a non-trivial solution, its determinant must be zero, resulting in the dispersion relation

$$\begin{aligned}
&-\sqrt{ks}\left[r^2(k(\mathscr{M}_c - \mathscr{M}_s\phi) + 2\phi + 1) + r(k(\mathscr{M}_c + \mathscr{M}_s(\phi+2)) + \mathrm{i}\mathscr{M}_ss - 1) + \mathrm{i}\mathscr{M}_ss\right] \\
&\quad + \left(k^2r(\mathscr{M}_c(r\phi+1) + \mathscr{M}_s(\phi+1)) + k\left(r^2\phi(\phi+1) - \mathrm{i}\mathscr{M}_ss(r\phi-1)\right) + 2\mathrm{i}rs\phi\right) \\
&\quad \times \frac{\sqrt{\pi}(r-1)}{(1-\mathrm{i})}\mathrm{e}^{(\mathrm{i}k(r\phi+1)^2/2s)}\left[1 - \mathrm{erf}\left(\frac{(1+\mathrm{i})\sqrt{k}(r\phi+1)}{2\sqrt{s}}\right)\right] = 0,
\end{aligned} \tag{4.10}$$

where $\phi = \sigma/k$ denotes the phase speed, $s = rS$ denotes a reduced shear parameter, and $\mathscr{M}_c = \mathscr{M} - \mathscr{M}_s$. As is the case for DL, (4.10) has two complex roots (owing to the quadratic power in ϕ) and we are only interested in the root with the largest real part, which determines the stability properties of the flame. The solution of (4.10) is obtained by a classical Newton method. First, one can easily verify that for $k = 0$ we have $\phi = 0$. But, this is not always the best starting point of the Newton method if we need to obtain the two roots of the solution, to ensure we are selecting the most unstable mode. To select an appropriate initial point in the iterative method, the most

reliable approach is to observe that for small k, the exponential and the error function in (4.10) are both very nearly one and zero, respectively. Then, one can solve the quadratic equation for ϕ (valid for small k to order $\sqrt{k}$) and obtain expressions for the two approximate roots. The first root behaves as $\phi \sim \sqrt{k}$ and the second as $\phi \sim 1/k$. From these initial conditions it is simple to trace the complete curves describing the two solutions of ϕ as a function of k. It turns out that it is always the first root that has the larger real part.

The current dispersion relationship can be compared with the DL relationship without shear but including curvature and strain, see Creta & Matalon (2011*b*) (they considered the case of a single Markstein number), which has solution

$$\phi = \{k(\mathscr{M}_c r + \mathscr{M}_s) + r - ([k(\mathscr{M}_c r + \mathscr{M}_s) + r]^2 - r[k\mathscr{M}_s(1-r) + r + 1] \times [k(2\mathscr{M}_c - \mathscr{M}_s(r-3)) + r - 1])^{1/2}\} / \{r[k\mathscr{M}_s(r-1) - (r+1)]\}. \quad (4.11)$$

Several distinguished limits will be discussed next to elucidate the effects of the different parameters in the solution. Then, we will consider a few prototypical situations of combustion of hydrogen, methane and propane with air, with Markstein numbers suggested by Clavin & Graña-Otero (2011).

4.1. *Limit of vanishing Markstein numbers*

First, we consider the limit of zero Markstein numbers which is analogous to the original DL instability result for a planar flame without shear. The dispersion relationship in this case is obtained by setting $\mathscr{M}_s = \mathscr{M}_c = 0$ in (4.10), giving

$$-\sqrt{ks}\left[r^2(2\phi+1) - r\right] + \left[k(r^2\phi(\phi+1)) + 2\mathrm{i}rs\phi\right] \times \frac{\sqrt{\pi}(r-1)}{(1-\mathrm{i})} \mathrm{e}^{(\mathrm{i}k(r\phi+1)^2/2s)} \left[1 - \mathrm{erf}\left(\frac{(1+\mathrm{i})\sqrt{k}(r\phi+1)}{2\sqrt{s}}\right)\right] = 0. \quad (4.12)$$

Figure 2 shows the behaviour of $\mathrm{Re}(\sigma)$ as a function of s, as well as the original DL curve ($s = 0$ limit), for $r = 1/7$. As can be seen, the main role of shear is to stabilize the flame at low wavenumbers (large wavelengths). The cross-over wavenumber, k_0, at which the flame becomes unstable depends on s and r and it can be obtained in principle by setting $\phi = \mathrm{i}\phi_i$ in (4.12) and solving for k. Figure 3 shows the behaviour of k_0 for different values of s and r. It is observed that the dependence on s is apparently linear while r changes the slope of these lines.

4.2. *Limit of vanishing density jump*

Another interesting limit is obtained by setting $r = 1 - \delta$ where $0 < \delta \ll 1$, analogously to the thermodiffusive approximation. The main item that must be considered carefully is the behaviour of $\mathscr{M}_s$ and $\mathscr{M}_c$ in this limit. It can be easily confirmed from Clavin & Graña-Otero (2011) that both Markstein numbers remain finite as $\delta \to 0$. Therefore, to leading order in δ, (4.10) becomes

$$-\sqrt{ks}\left[(k(\mathscr{M}_c - \mathscr{M}_s\phi) + 2\phi + 1) + (k(\mathscr{M}_c + \mathscr{M}_s(\phi+2)) + \mathrm{i}\mathscr{M}_s s - 1) + \mathrm{i}\mathscr{M}_s s\right] + (k^2(\mathscr{M}_c(\phi+1) + \mathscr{M}_s(\phi+1)) + k(\phi(\phi+1) - \mathrm{i}\mathscr{M}_s s(\phi-1)) + 2\mathrm{i}s\phi) = 0, \quad (4.13)$$

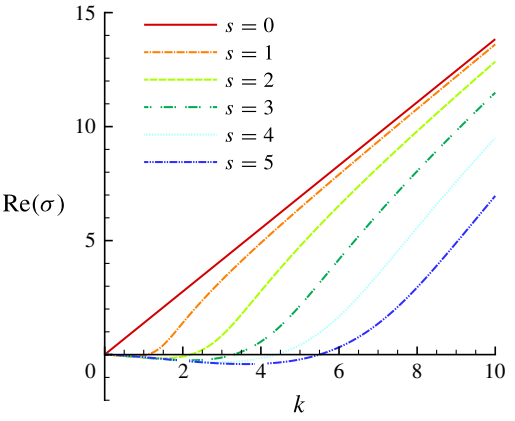

FIGURE 2. (Colour online) Classical Darrieus–Landau stability curves with shear (zero Markstein numbers) for $r = 1/7$.

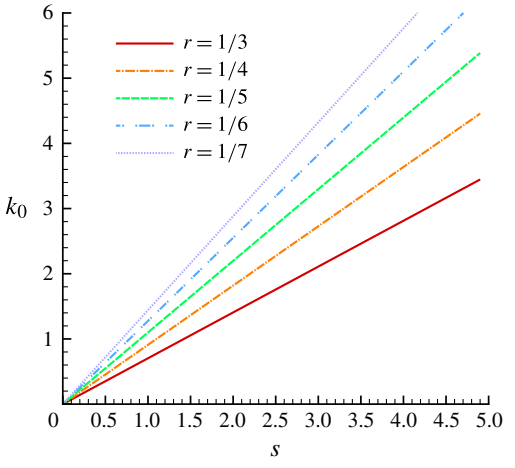

FIGURE 3. (Colour online) Dependence of k_0 on s for different r.

which can be solved explicitly for ϕ, giving

$$\phi = -(k(\mathscr{M}_s + \mathscr{M}_c) + \mathrm{i}s\mathscr{M}_s) = -(k\mathscr{M} + \mathrm{i}s\mathscr{M}_s). \tag{4.14}$$

This result is consistent with the same limit for the DL analysis without shear, indicating that the flame is stable for positive $\mathscr{M}$ and unstable for negative $\mathscr{M}$, and that it is density variation that makes the flame unstable for positive $\mathscr{M}$. Shear affects σ only through the imaginary term (phase speed) that plays no role in stability of the flame.

4.3. *Limit of strong density jump*

An interesting limit arises when the density jump across the flame is very large, as might be found in thermonuclear deflagrations. In this case, ρ_+ can be much smaller than ρ_-, resulting in the limiting case $0 < r \ll 1$. Note that it is possible to take the limit $r \to 0$ in the dispersion relation (which gives a finite result) but it is not

completely physical for the flow (it is a singular limit) because mass conservation will result in an infinite velocity in the burned side, see (3.1*b*).

The dispersion relation for this limit can be obtained by manipulating (4.10), which after some algebraic manipulations, gives

$$\sigma = \frac{1 - 2k\mathscr{M}_c - 3k\mathscr{M}_s - 2\mathrm{i}\mathscr{M}_s S}{2\mathscr{M}_s}. \tag{4.15}$$

The key technical detail in deriving the above equation is to observe that for large z we have

$$\mathrm{erf}(z) \approx 1 - \frac{\mathrm{e}^{-z^2}}{\sqrt{\pi} z}, \tag{4.16}$$

where

$$z = \frac{(1+\mathrm{i})\sqrt{k}(r\phi + 1)}{2\sqrt{rS}}, \tag{4.17}$$

with r approaching zero. Then the terms in the last line of (4.10) become

$$\frac{\sqrt{rS}(r-1)}{\sqrt{k}(1+r\phi)}, \tag{4.18}$$

which transforms the dispersion relation into a quadratic equation that can be solved explicitly for ϕ. This leads, after expansion in powers of r, to (4.15). One can also verify easily that by setting $S = 0$ in (4.15) the amplification factor agrees with the corresponding limit of (4.11) when $r \to 0$. The main observation from this (now simple) equation (4.15) is that shear does not affect the most unstable mode since it contributes a purely imaginary term and the amplification factor is identical to that of the DL instability without shear.

4.4. *Zero strain case*

This case corresponds to the original correction of Markstein to the DL analysis, where only curvature is accounted for in the problem, $\mathscr{M}_s = 0$ and $\mathscr{M}_c = \mathscr{M}$. The interest of this situation is that the dispersion relation can be rescaled by $\mathscr{M}$, by choosing $k \to \mathscr{M}k$ and $s \to rS\mathscr{M}$, and the result is therefore generic and equivalent to $\mathscr{M} = 1$. We focus mostly on the case $r = 1/7$ to discuss the qualitative properties of the solution. The results are similar for other sufficiently small values of r; the dependence of the solution on r is investigated in more general terms in figure 6 below. Figure 4 shows real and imaginary parts of the root of (4.10) with the larger real part for various reduced shear values and $r = 1/7$, as well as the DL amplification factor without shear, (4.11).

As is well known, the first term in (4.11) dominates at small wavenumbers while the second (stabilizing) term dominates at high wavenumbers. When comparing the effect of shear, one can verify that σ approaches the DL result as $s \to 0$ (as shown in figure 4*a*), which confirms that the analysis was carried out correctly. First, concentrating on the real part of σ and as the value of s increases, the curves move to the right and immediately introduce a gap of stability (negative $\mathrm{Re}(\sigma)$) at the smallest wavenumber, as shown in figure 2. At the same time, the peaks of the

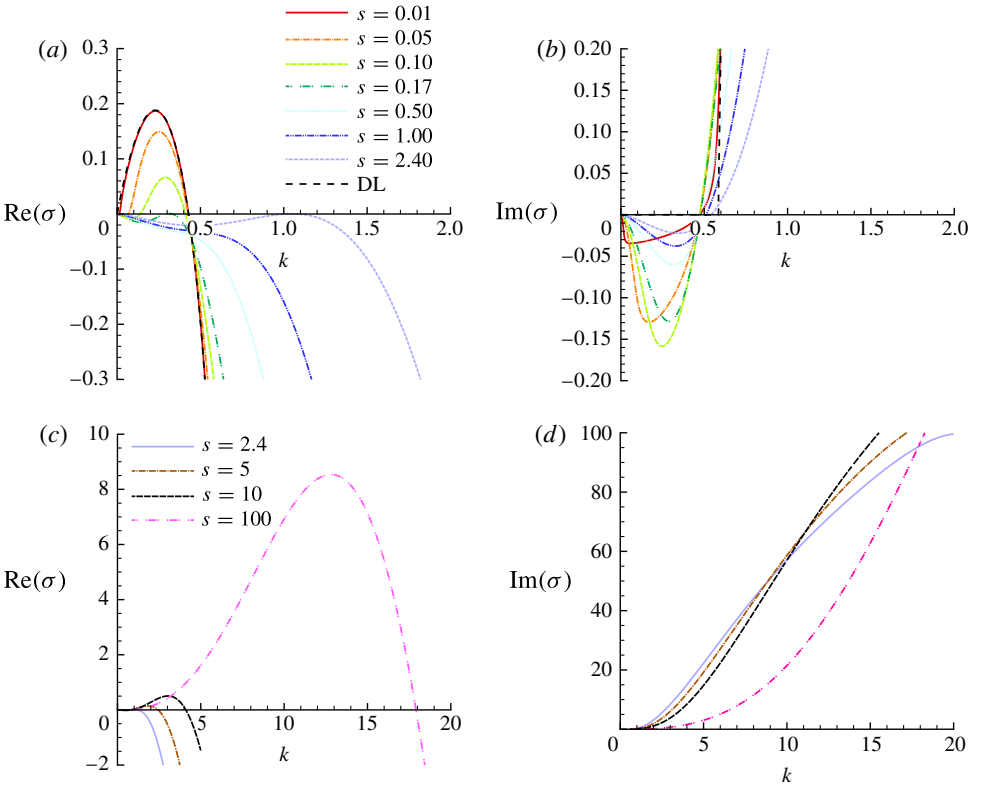

FIGURE 4. (Colour online) Real (*a,c*) and imaginary (*b,d*) values of σ with the larger real part as a function of reduced wavenumber for $\mathscr{M} = 1$, $r = 1/7$ and various s.

curves decrease and eventually they become completely negative at $s \approx 0.17$. Beyond that value of s, the flame is stable at all wavenumbers. As s continues to increase, the curve bends up and first becomes tangent to the $\sigma = 0$ axis at $s \approx 2.4$. Beyond this value of s, we recover a bell-shaped curve with a positive peak at a location dependent on the value of s and a further decay towards negative values for growing wavenumber (a consequence of the stabilizing role of curvature), see figure 4(*c*). Second, figure 4(*b*) shows that the magnitude of the imaginary part of σ is negative (being zero for DL in the unstable range of wavenumbers) for low s while it becomes positive for large s. The consequence of σ not being purely real is that the solution will have a travelling wave character, see (4.1).

To determine the speed of the travelling wave character of the solution, we investigate the phase speed $c = \mathrm{Im}(\phi)$ in figure 5. It can be seen that the phase speed is negative for small s and positive for large s. The latter is consistent with the direction of the imposed shear, but the former may appear counterintuitive, being in the opposite direction. In fact, we can see in the distinguished limit $r \to 1$, (4.14), that the expected result is to have a negative phase speed (assuming $S > 0$) for $\mathscr{M}_s > 0$. Here, one may note the fact that the results in figure 5 refer to $\mathscr{M}_s = 0$ and therefore (4.14) predicts zero phase speed in this case. To address this difficulty, (5.1) below shows the result for a Kelvin–Helmholtz interface between two fluids of different densities using the same reference conditions as in the present flame. This would be the limit of high shear, where the self-propagation feature of the premixed

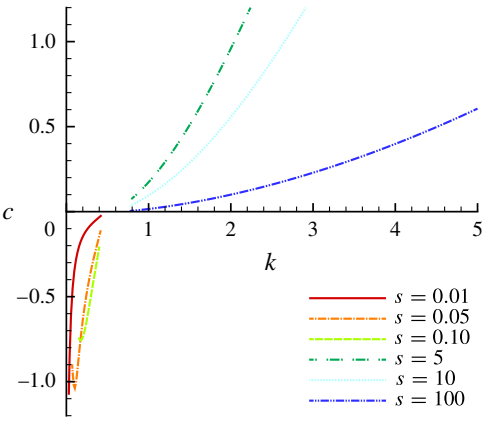

FIGURE 5. (Colour online) Phase speed c as a function of wavenumber for $\mathscr{M} = 1$, $r = 1/7$ and various s. The phase speed is only plotted in the regions where $\mathrm{Re}(\sigma) > 0$.

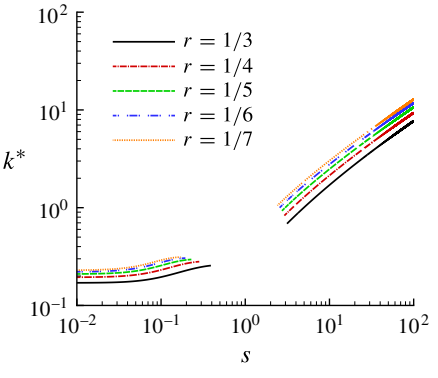

FIGURE 6. (Colour online) Most unstable wavenumber as a function of s for different r and $\mathscr{M} = 1$.

flame is negligible in comparison with the effect of shear. Since $r < 1$, the phase speed is indeed negative for the Kelvin–Helmholtz mode and this is irrespective of the values of Markstein numbers. It is, therefore, the positive phase speed behaviour of the flame in the presence of large shear that is unexpected, and it must be the result of the nonlinearities in the dispersion relation that couple with the finite heat release. In other words, the phase speed is determined by the sign of $r - 1$, as in (5.1), but in a manner controlled by s.

Figure 6 shows the wavenumber of the most unstable mode, k^* (at the peak of $\mathrm{Re}(\sigma)$), as a function of the reduced shear parameter s for different values of r relevant to typical combustion: $1/7 \leqslant r \leqslant 1/3$ (other lower values of r give similar results). Figure 6 shows that in all cases one observes that the 'island' of stability, whose precise boundaries depend on the value of r, is present. This island appears to exist for all practical values of r and therefore should be relevant in applications when premixed flames propagate in regions of shear since the flame may experience different stabilizing–destabilizing conditions depending on the local value of s.

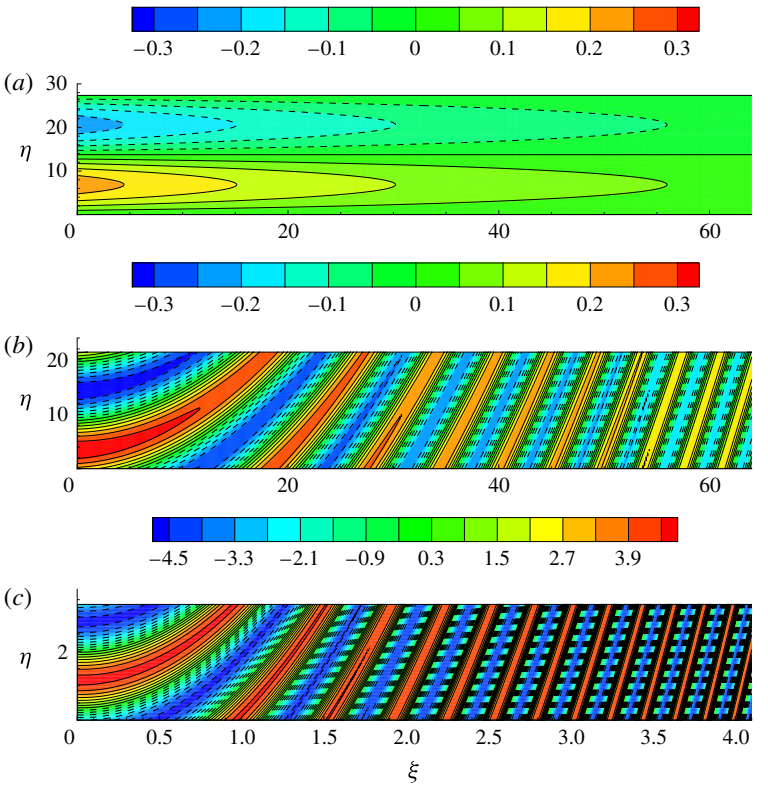

FIGURE 7. (Colour online) Vorticity for $r = 1/7$ at the most unstable wavenumber for $s = 0$ (a) (DL with curvature effect only), $s = 0.1$ (b) and $s = 5$ (c).

To conclude, figure 7 shows isocontours of vorticity for DL, with curvature stabilization only, and $s = 0.1$ and 5 in the post-flame region (downstream); vorticity is zero upstream for all values of s. The vorticity can be calculated explicitly and results in the following formula (valid for $\mathscr{M} = 1$):

$$\begin{aligned}\tilde{\omega} &= \left(\frac{\partial \tilde{v}}{\partial \xi} + \mathrm{i}k\tilde{u}\right)\mathrm{e}^{-\mathrm{i}k\eta} \\ &= -\frac{2(1-\mathrm{i})\sqrt{sk}}{\sqrt{\pi}}\exp\left[-k\left((\xi+\mathrm{i}\eta) + \mathrm{i}((1-r\phi+\mathrm{i}s\xi)^2/2s)\right)\right], \end{aligned} \tag{4.19}$$

which excludes the temporal modulation since the complete vorticity is travelling with phase speed c. Figure 7 shows the real part of (4.19). The main change induced by shear is the tilting of the isocontours in the direction of the imposed shear (upwards in these figures). The picture for low s is similar to that at high s but there is a larger density of ripples (smaller wavelengths) in the flame-normal direction while the transverse wavelength depends on s, as can be seen in figure 6. Furthermore, the complete vorticity solution will be traveling at the phase speed c (downwards or upwards depending on s) and being amplified exponentially in time (since we are only concerned with the unstable mode). Note that the vorticity decays to zero at large ξ but at a rate that is slower than that of the DL solution.

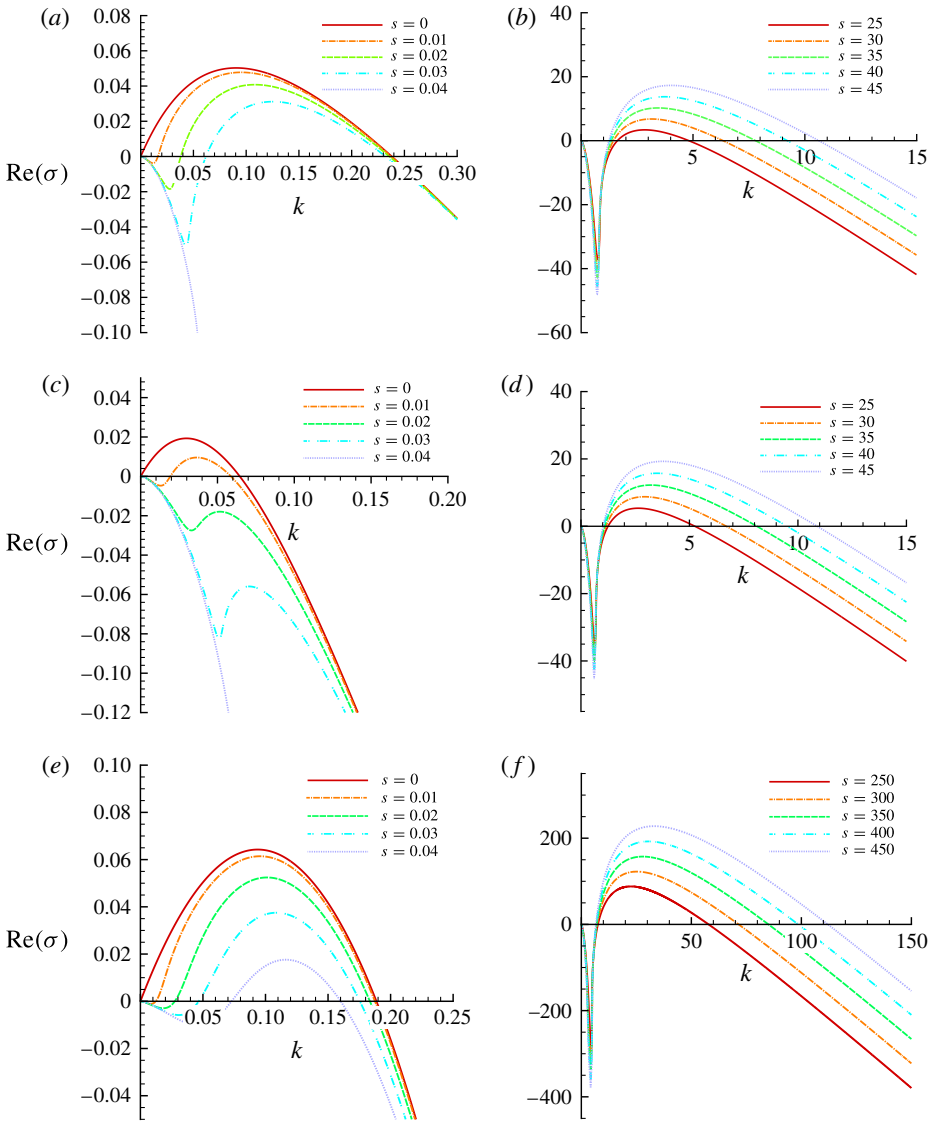

FIGURE 8. (Colour online) Amplification factors for a prototypical hydrogen–air flame (*a,b*), lean methane–air flame (*c,d*) and lean propane–air flame (*e,f*).

4.5. *Behaviour in prototypical combustion conditions*

We consider now the dispersion relation solution as a function of s for several Markstein numbers discussed in Clavin & Graña-Otero (2011) as representative of combustion of low-Lewis-number mixtures corresponding to hydrogen–air and close to unity-Lewis-number mixtures characteristic of hydrocarbon combustion.

Figure 8 shows dispersion relation results for a prototypical rich hydrogen–air flame with $\mathscr{M}_s = 3$ and $\mathscr{M}_c = -2.5$ (*a,b*), a prototypical lean methane flame with $\mathscr{M}_s = 3.5$ and $\mathscr{M}_c = 1.5$ (*c,d*) and a lean propane flame with $\mathscr{M}_s = 0.5$ and $\mathscr{M}_c = 1.5$ (*e,f*), all at $r = 1/6$. In all cases, we reproduce qualitatively the result in the previous section. Starting at $s = 0$ and with increasing s, the flame becomes less unstable and eventually

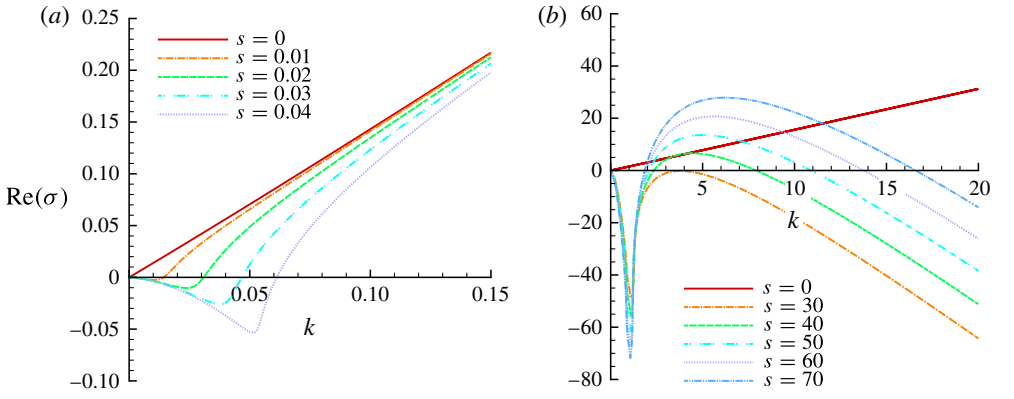

FIGURE 9. (Colour online) Amplification factors for a flame with $\mathscr{M}_s = 2$, $\mathscr{M}_c = -5$ and $r = 1/6$.

it stabilizes completely at some small value of s. But, if s continues to increase, the flame becomes unstable again within a range of wavenumbers, that grows with increasing s, as seen in all the figures.

4.6. *Negative Markstein numbers*

Finally, we investigate the effect of shear on flames with negative Markstein numbers. Traditionally, this regime is not often discussed because the flame is absolutely unstable (at all wave modes). Also note that for $s = 0$ and negative strain, Markstein number from equation (4.11) is singular at the finite value of $k = (r+1)/((r-1)\mathscr{M}_s)$. This is presumably an intrinsic limitation of the description based on a strictly zero flame thickness when $s = 0$.

In the present configuration, the stabilization introduced by shear implies that negative Markstein number flames can become conditionally unstable. This is clearly observed in figure 9 where the amplification factor for a flame with $\mathscr{M}_s = 2$ and $\mathscr{M}_c = -5$ is shown. This flame has negative Markstein number for the curvature term and positive Markstein number for the strain term in the flame speed relationship. We observe a stable region for small s at low wavenumbers, as before, but a conditionally stable situation at higher s. This latter regime is analogous to the behaviour observed for positive Markstein numbers before because the stabilization effect of strain is still present. Note that the corresponding amplification factor for $s = 0$ is unconditionally unstable for this flame. Figure 10 shows the result for a flame with both Markstein numbers being negative, $\mathscr{M}_s = -2$ and $\mathscr{M}_c = -5$, where it is seen that the flame is conditionally unstable. The amplification factor for small shear is very similar to that of the $s = 0$ case (small shear does not stabilize the flame). We also do not find a singularity of the amplification factor for negative Markstein numbers when s is larger than approximately 0.32 (for this flame) and the flame seems to be conditionally unstable always.

5. Discussion: the second region of instability

As discussed in the preceding sections, all flames are conditionally unstable for sufficiently high shear, even with negative Markstein numbers. The reasons this happens is unclear. One might conjecture that in this limit the flame propagation

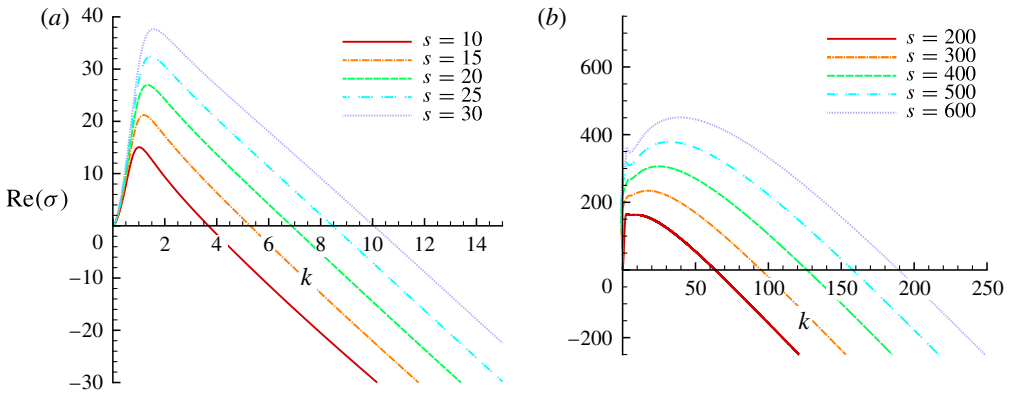

FIGURE 10. (Colour online) Amplification factors for a flame with $\mathscr{M}_s = -2$, $\mathscr{M}_c = -5$ and $r = 1/6$.

speed is negligible and the interface is therefore Kelvin–Helmholtz unstable with a density jump given by heat release. This situation would correspond to that of a sheared interface of two immiscible fluids of different densities. Now, a straightforward stability analysis, see Drazin & Reid (1981), gives an amplification factor of

$$\sigma = \frac{2\mathrm{i}(r-1)S}{(r+1)}, \tag{5.1}$$

which corresponds to a neutrally stable interface. Therefore, it is not a Kelvin–Helmholtz instability that dominates at high shear, but a truly intrinsic interaction of the flame dynamics with shear.

6. Conclusions

A linear stability analysis of the behaviour of a laminar premixed flame subjected to a constant lateral shear has been carried out analytically. The interest of this problem resides in applications where a premixed flame can propagate into regions of free shear flow, which can alter the flame behaviour. The analysis extends the classical Darrieus–Landau instability analysis to include the stabilization effect produced by flame curvature and strain. The dispersion relation is obtained and its roots are discussed in detail. The stability analysis indicates that the flame show three regimes as a function of a reduced shear parameter. At low shear, the behaviour is analogous to Darrieus–Landau analysis, albeit with some correction, the flame becoming progressively more stable as shear increases. Further increase in shear results in unconditionally stable behaviour. Finally, as shear continues to increase, the flame becomes unstable again with higher amplification rate and at lower wavelengths than the low shear case. All solutions are stable at sufficiently high wavenumbers due to curvature and strain stabilization. This island of stability is observed at all heat release levels considered.

Acknowledgements

This work was supported in part by the Department of Energy, National Nuclear Security Administration, under award no. DE-NA0002382 and the California Institute

of Technology. We also thank M. Matalon for the comments on the first draft of the manuscript.

REFERENCES

ALDREDGE, R. C. 1996 Premixed flame propagation in a high-intensity, large-scale vortical flow. *Combust. Flame* **106** (1), 29–40.

ASHURST, W. T. & SIVASHINSKY, G. I. 1991 On flame propagation through periodic flow fields. *Combust. Sci. Technol.* **80** (1–3), 159–164.

AUDOLY, B., BERESTYCKI, H. & POMEAU, Y. 2000 Réaction diffusion en écoulement stationnaire rapide. *C. R. Acad. Sci. Paris* II **328** (3), 255–262.

BERESTYCKI, H. & SIVASHINSKY, G. I. 1991 Flame extinction by periodic flow field. *SIAM J. Appl. Maths* **51** (2), 344–350.

BRAILOVSKY, I. & SIVASHINSKY, G. 1993 On quenching of the reaction wave moving through spatially periodic shear flow. *Combust. Sci. Technol.* **95** (1–6), 51–60.

BRAILOVSKY, I. & SIVASHINSKY, G. 1995 Extinction of a nonadiabatic flame propagating through spatially periodic shear flow. *Phys. Rev.* E **51** (2), 1172–1183.

BUCKMASTER, J. 1977 Slowly varying laminar flames. *Combust. Flame* **28**, 225–239.

CLAVIN, P. & GRAÑA-OTERO, J. C. 2011 Curved and stretched flames: the two Markstein numbers. *J. Fluid Mech.* **686**, 187–217.

CLAVIN, P. & WILLIAMS, F. A. 1982 Effects of molecular diffusion and of thermal expansion on the structure and dynamics of premixed flames in turbulent flows of large scale and low intensity. *J. Fluid Mech.* **116**, 251–282.

CRETA, F. & MATALON, M. 2011*a* Propagation of wrinkled turbulent flames in the context of hydrodynamic theory. *J. Fluid Mech.* **680**, 225–264.

CRETA, F. & MATALON, M. 2011*b* Strain rate effects on the nonlinear development of hydrodynamically unstable flames. *Proc. Combust. Inst.* **33**, 1087–1094.

DARRIEUS, G. 1938 Propagation d'un front de flamme. In *La Téchnique Moderne and Congrés de Méchanique Appliquée*, Cambridge University Press (1945).

DRAZIN, P. G. & REID, W. H. 1981 *Hydrodynamic Stability*. Cambridge University Press.

DRISCOLL, J. F. 2008 Turbulent premixed combustion: flamelet structure and its effect on turbulent burning velocities. *Prog. Energy Combust. Sci.* **34** (1), 91–134.

HAWKES, E. R., CHATAKONDA, O., KOLLA, H., KERSTEIN, A. R. & CHEN, J. H. 2012 A petascale direct numerical simulation study of the modelling of flame wrinkling for large-eddy simulations in intense turbulence. *Combust. Flame* **159** (8), 2690–2703.

JOULIN, G. & SIVASHINSKY, G. 1994 Influence of momentum and heat losses on the large-scale stability of quasi-2d premixed flames. *Combust. Sci. Technol.* **98** (1–3), 11–23.

KAGAN, L. & SIVASHINSKY, G. 2000 Flame propagation and extinction in large-scale vortical flows. *Combust. Flame* **120** (1), 222–232.

KAGAN, L., SIVASHINSKY, G. & MAKHVILADZE, G. 1998 On flame extinction by a spatially periodic shear flow. *Combust. Theor. Model.* **2** (4), 399–404.

KORTSARTS, Y., KLIAKHANDELER, I., SHTILMAN, I. & SIVASHINSKY, G. 1998 Effects due to shear flow on the diffusive-thermal instability of premixed gas flames. *Q. Appl. Maths* **56** (3), 401–412.

LANDAU, L. D. 1945 On the theory of slow combustion. *Acta Physicochim. USSR* **19**, 77–85.

LIPATNIKOV, A. N. & CHOMIAK, J. 2010 Effects of premixed flames on turbulence and turbulent scalar transport. *Prog. Energy Combust. Sci.* **36** (1), 1–102.

MARKSTEIN, G. H. 1964 *Nonsteady Flame Propagation*. Macmillan.

MATALON, M. 1983 On flame stretch. *Combust. Sci. Technol.* **31** (3–4), 169–181.

MATALON, M. 2007 Intrinsic flame instabilities in premixed and nonpremixed combustion. *Annu. Rev. Fluid Mech.* **39**, 163–191.

MATALON, M. & MATKOWSKY, B. J. 1982 Flames as gas-dynamic discontinuities. *J. Fluid Mech.* **124**, 239–259.

PELCÉ, P. & CLAVIN, P. 1982 Influence of hydrodynamics and diffusion upon the stability limits of laminar premixed flames. *J. Fluid Mech.* **124**, 219–237.

PETERS, N. 2010 *Combustion Theory*. RWTH Aachen University (CEFRC Summer School).

SEARBY, G. & CLAVIN, P. 1986 Weakly turbulent, wrinkled flames in premixed gases. *Combust. Sci. Technol.* **46** (3–6), 167–193.

SIVASHINSKY, G. I. 1976 On a distorted flame front as a hydrodynamic discontinuity. *Acta Astron.* **3** (11), 889–918.

SIVASHINSKY, G. I. 1977 Nonlinear analysis of hydrodynamic instability in laminar flames. I. Derivation of basic equations. *Acta Astron.* **4** (11), 1177–1206.

SIVASHINSKY, G. I. 1983 Instabilities, pattern formation, and turbulence in flames. *Annu. Rev. Fluid Mech.* **15** (1), 179–199.

SIVASHINSKY, G. I. 1990 On the intrinsic dynamics of premixed flames. *Phil. Trans. R. Soc. Lond.* A **332** (1624), 135–148.

WILLIAMS, F. A. 1985 *Combustion Theory: The Fundamental Theory of Chemical Reacting Flow Systems*. Benjamin Cummings.